Title	Dose-reduction effects of vehicles against gamma radiation in the case of a nuclear accident
Author(s)	Takahara Shogo, Watanabe Masatoshi, Hirouchi Jun, Iijima Masashi, Munakata Masahiro
Citation	Health Physics, 114(1), p.64-72
Text Version	Author's Post-print
URL	https://jopss.jaea.go.jp/search/servlet/search?5059151
DOI	https://doi.org/10.1097/HP.0000000000000729
Right	© 2018 Health Physics Society. This is a non-final version of an article published in final form in Health Physics, 114(1), p.64-72;2018

Dose-reduction effects of vehicles against gamma radiation in the case of a nuclear accident

Shogo TAKAHARA[*], Masatoshi WATANABE[*], Jun HIROUCHI[*], Masashi IIJIMA[*], and Masahiro MUNAKATA[*]

Corresponding Author:

Shogo TAKAHARA

2-4 Shirane, Shirakata, Tokai-mura, Naka-gun, Ibaraki 319-1195, Japan

Tel +81-29-6139 Fax +81-29-6147

E-mail takahara.shogo@jaea.go.jp

[*]Japan Atomic Energy Agency, Nuclear Safety Research Center, 2-4 Shirane, Shirakata, Tokai-mura, Naka-gun, Ibaraki 319-1195, Japan;

ABSTRACT

Self-evacuation by a private vehicle is one of the most commonly used methods of public evacuation in the case of a nuclear accident. The aim of this paper is to evaluate the dose-reduction effects of vehicles. To achieve this aim, a model for calculating the dose reduction factor was developed based on the actual shape and weight of Japanese vehicles. This factor is defined as the ratio of dose rate inside a vehicle to that outside. The model was developed based on weight of vehicle to take into account the dose-reduction effects due to not only the steel plate of vehicle body but also the other all assemblies. In addition to model calculation, we evaluated the dose reduction factors by actual measurements in the areas contaminated by the Fukushima Daiichi Nuclear Power Plant accident. A comparison between the simulated and the measured results revealed that the dose reduction factors obtained using the developed models were in good agreement with the results of actual measurements. Using this model, we also evaluated the dose reduction factors for cloudshine and groundshine in the case of a nuclear accident. The evaluations were performed for four vehicle models whose weights were 800–1930 kg. The dose reduction factor for cloudshine with photon energy of 0.4–1.5 MeV was 0.66–0.88, and that for groundshine from ^{137}Cs was 0.64–0.73. Although these results were obtained under the assumption that ^{137}Cs is placed only the ground surface, according to our considerations, if ^{137}Cs migrated into the ground corresponding to the relaxation mass depth of 10 g cm^{-2}, the dose reduction factors would be almost 8% less than those for the ground surface.

KEYWORDS: nuclear accident, evacuation, vehicle, dose reduction effect

INTRODUCTION

A major nuclear accident with the release of radioactive materials can expose people living in the affected areas to significant doses of radiation. For many types of emergencies, radiation exposure rates are the greatest immediately after the onset of the release of radioactive materials from a reactor core into the environment. In such situations, protective actions need to be taken promptly to prevent radiation-induced health effects and to reduce their risks to people. However, in real time, there may be little time to implement some of the considerations of such protective actions based on detailed exposure assessments. It is therefore necessary to optimize the overall protection strategy by taking into account the dose-reduction effect of each individual action and the compound effect of such actions in advance of an accident.

Evacuation is one of the typical protective actions in such a situation, and it is assumed to be completely effective because radiation dose from the accident is considered zero as soon as the entire population of the contaminated area has been evacuated. However, if the timing of evacuation is delayed or misjudged, the evacuees cannot avoid passing through the radioactive plume or through areas contaminated by radionuclide deposits. Therefore, the potential doses from such exposure sources during evacuations have to be assessed and considered when optimizing the evacuation strategy in the case of a nuclear accident. In general, evacuation is achieved by a combination of self-evacuation and transport organized by the authority. In particular, in the light of past experiences from the Three Mile Island accident (Cutter and Barnes, 1982) and the Fukushima Daiichi Nuclear Power Plant accident (NAIIC, 2012; Hiroi, 2014), self-evacuation has been in focus recently. For example, in Japan, private vehicles were widely used by the public for self-evacuation in the aftermath of the nuclear emergency, and this was accounted for in the response plan of the local government*. Although some jurisdictions would arrange transportation using existing public transport infrastructure, many acknowledge that a large proportion of citizens will choose to evacuate using their own vehicles (OECD/NEA/CRPPH, 2012). Therefore, the dose-reduction effect of vehicles is a key element for optimizing the overall protective strategy, and its impact on evacuees should be evaluated.

Studies have reported on the dose-reduction effect of vehicles (Burson and Profio, 1977; Lauridsen and P-Hedemann, 1983), but these studies were performed a few decades ago in European countries. Therefore, further considerations are needed to generate meaningful information for preparing a nuclear emergency

strategy considering actual vehicles using state-of-art techniques in Japan. In the present study, to achieve this aim, we first developed a model for calculating dose-reduction factor (DRF) based on the actual shape and weight of Japanese vehicles. The DRF was used for evaluating the dose-reduction effects of vehicles, and it was defined as the ratio of the dose rate inside a vehicle to that outside the vehicle. In addition to the model calculation, we evaluated DRFs by actual measurements in the areas contaminated by the Fukushima accident. Then, by using the developed model, we also evaluated DRFs for the following two exposure pathways in the case of a nuclear accident: (i) external exposure from radioactive clouds released from a nuclear power plant (hereinafter cloudshine) and (ii) radionuclides deposited onto the ground surface (hereinafter groundshine).

DEVELOPMENT OF VEHICLE MODEL

Calculation method

To evaluate DRFs of the vehicle models, the ambient equivalent dose rate inside and outside the models were calculated using MCNP5 (Monte Carlo calculation code) (X-5 Monte Carlo Team, 2003) and ENDF/B-VI Release 8 cross-section data (White, 2003). For each vehicle model, photon flux was computed and converted using the dose conversion coefficients adopted by the International Commission on Radiological Protection publications 74 (ICRP, 1996). For measuring photon flux, point detectors were used. In addition, calculations were made under the condition that statistical relative error be lower than about 1%.

The DRF evaluations were performed considering the contributions of deposited ^{134}Cs and ^{137}Cs. The ^{134}Cs:^{137}Cs ratio was assumed based on UNSCEAR report (UNSCEAR, 2014), and the value of 0.23 was used as of October 2015. These radioactive cesium isotopes were deposited uniformly within a radius of 500 m from the vehicle model. The vehicle model was located at the center of a half-sphere with a radius of 1000 m filled with air. Ground soil was considered up to 1 m below the ground surface, and the soil density was assumed to be 1.6 g cm^{-3} according to a previous study (Eckerman and Ryman, 1993). To consider the influence of radionuclide migration into the ground, we assumed that radioactive cesium is placed at a depth of 0 and 6.3 cm. These depths, considering soil density of 1.6 g cm^{-3}, correspond to relaxation mass depths β = 0 g cm^{-2} and 10 g cm^{-2}, respectively.

Calculation model of vehicle

The vehicle models were developed based on the actual shapes and the weights of the vehicles Mira, Vitz, Wish, and Alphard, and which were obtained from the respective inspection certificates. **Table 1** summarizes these data. The length, width, and height of vehicle bodies, as well as minimum ground clearance were collected. The distance from the bottom of vehicle model to the ground surface was considered the minimum ground clearance in our calculations. **Figure 3** shows a schematic illustration of the vehicle model developed based on these shape data. The shape of the vehicle model was assumed to be rectangular. Windows of the vehicle model were assumed to be rectangular and located at 10 cm below the ceiling of vehicle. The length of the side window was determined based on the interior length of the vehicle. Window height was obtained by averaging the heights of the four windows (front, rear, and side).

Furthermore, we collected the weight data of the four vehicles to determine body-thickness of each vehicle model. The thicknesses of the vehicle models were evaluated on the assumption that the vehicle bodies are made of steel plates, according to following eqn (1):

$$M - M_0 = \rho \cdot d \cdot S, \quad (1)$$

where, M is the weight of vehicle, M_0 is the weight of ceiling and windows, ρ is the density of steel (7.8 g cm^{-3}), d is the thickness of vehicle model, and S is the surface area of vehicle bodies excluding the ceiling and windows. Here the thickness of the ceiling of the vehicle body was assumed to be 0.08 cm based on the information provided by a Japanese automaker**. In addition, the thickness of window was determined based on a previous study (Ko, 2009), and the value of 0.36 cm was used for our model. The value of 2.4 g cm^{-3} was used for the density of windows.

In addition, the actual shape of the vehicle body is not rectangular because the corners of vehicle body are rounded, and the vehicle body has a slope to allow drivers and passengers to see the outside from the inside. If we take into account these aspects, the surface area of the actual vehicle is smaller than that of vehicle model built herein. To correct this point, the side areas of the rectangular models of Mira, Vitz, Wish, and Alphard were reduced by 3.8%, 15.3%, 12.0%, and 10.1%, respectively. Along similar lines, factors of 3.8%, 3.8%, 2.0%, and 2.0% were used for modeling ceiling areas of Mira, Vitz, Wish, and Alphard, respectively. As a result of the evaluations, the thicknesses of the vehicle models, except for ceiling, of Mira, Vitz, Wish, and Alphard

were 0.70 cm, 0.78 cm, 0.86 cm, and 0.93 cm, respectively.

The dose-reduction effects were evaluated by using DRFs, which were calculated as the ratio of the ambient equivalent dose rate inside a vehicle to that outside. The DRF calculations were performed for a representative point located 20 cm below the center of the vehicle model. In addition, to evaluate the variability due to difference in detector position, we performed calculations for six additional detection points, as shown in **Fig. 3**. These detectors were located at a distance of 50 cm front/rear from the representative point, distance of 20 cm up/down, and 40 cm left/right. Moreover, to evaluate the difference in the DRFs due to the difference in the mass density thickness between the windows and the steel plates, an additional detector was installed above the representative point at the same height of the center of the windows.

Experimental

To validate a vehicle model for evaluating the dose-reduction effects in the case of a nuclear emergency, we performed actual measurements of the ambient dose equivalent rates inside and outside the vehicles. The measurements were performed in a sports field located in Futaba Town in Fukushima prefecture on October 2015. This place is included in the list of areas where it is expected that the residents have difficulties in returning for a long time. In addition, a pilot decontamination program had been conducted at this location between 9 December 2013 and 23 January 2014. The decontamination was performed by stripping a thin layer of the topsoil and covering the exposed ground with uncontaminated soil (Ministry of Environment, 2014). **Figure 1** shows an overhead view of the measurement location. The latitude and longitude of the measurement location was 37°25'55"N 140°59'23"E.

The ground surface of this place was bare, and **Fig. 2** shows the radiation dose rate measured at a height of 1 m from the ground surface. The ambient equivalent dose rate increased along the X (only positive X direction) and the Y directions (both positive and negative direction) because there are some contaminated sources outside of the measurement location, such as contaminated forest, tufts of grass so on, in this direction. Average value of the radiation dose rate in measurement location is 1.85 μSv h^{-1}. According to measurement results by Fukushima prefecture (Fukushima Prefecture, 2010), the radiation dose rate measured before the Fukushima accident was 0.05 μSv h^{-1} in Futaba town. As described above, our measurements were performed

on October 2015, and this means 55 month passed after the accident. Therefore, the contributions from short-lived radionuclides decrease, and the most contributing radionuclides were ^{134}Cs and ^{137}Cs. The effective photon energy, which is defined in eqn (4), from ^{134}Cs and ^{137}Cs is 0.68 MeV and 0.66 MeV, respectively.

The vehicles were placed at the original point shown in **Figs. 1** and **2**. The measurements were performed using the following eight vehicles, which are widely used in Japan: Mira (Daihatsu Motor Co., Ltd), Vitz, Porte, Prius, Succeed, Wish, Alphard, and Vellfire (Toyota Motor Corporation, Tokyo, Japan). A NaI(Tl) scintillation survey meter (TCS-171B, Hitachi-Aloka Medical, Ltd., Tokyo, Japan) was used for measuring the ambient equivalent dose rate. The DRFs were evaluated as the ratio of the ambient equivalent dose rate measured inside a vehicle to that measured at a height of 1 m above the ground at the original point in the measurement location. For the measurements inside the vehicles, the survey meter was placed 15 cm above the driver's seat, as done in a previous study (Lauridsen and P-Hedemann, 1983).

Comparison of DRFs between actual measured value and value obtained from calculation model

Figure 4 shows the results of these DRF evaluations. The error bars in this figure are attributed to the spatial variability in detecting points inside a vehicle model in our evaluations. The DRFs obtained from the actual measurements ranged from 0.54 to 0.65, and they decreased with increasing vehicle weight. As shown in this figure, the DRFs evaluated using the vehicle models for β = 0 g cm^{-2} and 10 g cm^{-2} have the similar tendency with the results of the measured values, which ranged from 0.65 to 0.74 and 0.59 to 0.68, respectively. When the migration of radiation sources into the ground was taken into account in the model calculations, the gamma-ray intensity at the detection points decreased owing to attenuation effects of the soil layer. Thus, the corresponding ambient equivalent dose rate and DRF are lower than those calculated for β = 0 g cm^{-2}.

As compared to the actual measurements, the DRFs for β = 0 g cm^{-2} tended to be higher than the actual measured values, even when considering the variability at detection points inside a vehicle model. By contrast, in the case of the DRFs for β = 10 g cm^{-2}, considering the influence of spatial variability at the detection points, the evaluated values are close to the measured values within an error of a few percent. Matsuda and Saito (2016) reported the depth profile of the Fukushima accident-derived ^{137}Cs in Fukushima prefecture, and the value of 8.51 g cm^{-2} was observed as the maximum at the relaxation mass depth in locations that were not decontaminated as of September 2015.

However, Matsuda and Saito (2016) also pointed out that the relaxation mass depth exceeded 10 g cm^{-2} in the areas where decontamination was performed. As mentioned in the experimental section, the measurement location in our study was decontaminated after the accident. Therefore, according to Matsuda and Saito (2016), the relaxation mass depth in the measurement location in the present study is expected to exceed 10 g cm^{-2}, and this characteristic of depth distribution can explain well the results shown in **Fig. 4**. Consequently, it was confirmed that the DRFs evaluated from the vehicle model developed in the present study are in good agreement with the measured ones.

APPLICATION OF VEHICLE MODEL FOR EVALUATING DOSE-REDUCTION EFFECTS DUE TO VEHICLE IN CASE OF A NUCLEAR EMERGENCY

Accident scenarios and photon energy in case of a nuclear accident

Based on the vehicle models developed in the present study, we assessed the DRFs for cloudshine and groundshine. Calculations of the reduction factors for cloudshine were performed under the assumption that a vehicle is in submersion in radioactive materials. In this study, we assessed the DRFs for photon energies derived from a previous study on severe accidents (Homma et al., 2000) and from actual data on the Fukushima Daiichi Nuclear Power Plant accident (NERHGJ, 2011; Nishihara et al., 2012).

Average energy of gamma rays from exposure pathway j, E_j, is calculated as follows:

$$E_j(t) = \frac{\sum_i C_{i,j}(t) \cdot E_i}{\sum_i C_{i,j}(t)}, \quad (2)$$

where $C_{i,j}$ is the attributable fraction of radionuclide i to the ambient equivalent dose rate from exposure pathway j, and E_i is the effective energy of gamma rays released from radionuclide i.

$C_{i,j}$ can be represented in the following form using the activity of radionuclide i related to the exposure pathway j, $A_{i,j}$, and $k_{i,j}$ is the effective dose coefficient of radionuclide i from exposure pathway j;

$$C_{i,j}(t) = \frac{k_{i,j} \cdot A_{i,j}(t)}{\sum_i k_{i,j} \cdot A_{i,j}(t)}. \quad (3)$$

E_i is expressed as follows;

$$E_i = \frac{\sum_k r_{i,k} \cdot E_{i,k}}{\sum_k r_{i,k}}, \quad (4)$$

where $r_{i,k}$ is the fractional yield of a gamma ray produced per fission of radionuclide i. k is the index of the

decay process that photons with energy $E_{i,k}$. The radionuclide progeny yielded by these released fission products and the fractional yield of gamma ray, $r_{i,k}$, were determined based on IAEA TECDOC 1162 and Radioisotope pocket data book (IAEA,2000; Japan Radioisotope Association, 2011).

Table 2 shows the activity of radionuclide *i* released from a nuclear reactor based on the inventory in the nuclear reactor and the release fraction of each radionuclide for each accident scenario. The values shown in this table are normalized by the activity of ^{137}Cs for each accident scenario. The calculations of $C_{i,j}$ for cloudshine were performed considering the contribution of all 21 radionuclides listed in this table. By contrast, those for groundshine were performed without considering the contributions of noble gases. The inventory of these radionuclides in the nuclear reactor and the release fraction into the environment were determined according to a previous study and based on experiences from the Fukushima accident (Homma et al., 2000; NERHGJ, 2011; Nishihara, 2012). From a previous study on severe accidents (Homma et al., 2000), we decided to use three representative accident scenarios in terms of the amount of radionuclides released and the importance of planning for emergency preparedness. A part of these three scenarios was also used in the past as consideration for a nuclear emergency response plan in Japan (JAEA, 2012).

These scenarios were characterized from the aspect of plant damage state and containment failure mode. First, we selected an accident that could occur if the scram system fails to work during a reactor event and containment failure occurs through the drywell. This type of accident, called TC-DWF hereinafter, is one of the worst-case accidents, and large amounts of radioactivity are released rapidly after reactor shutdown. In addition, we considered a transient accident with the loss of all emergency core cooling system injections, including small break LOCA (called TQUV hereinafter). If containment failure occurs through the drywell (called TQUV-DWF hereinafter), such an accident could release radioactivity as much as that in TC-DWF. Therefore, this type of accident is also important when preparing a nuclear emergency response plan. Finally, we considered the TQUV scenario with a containment vent (called TQUV-CV hereinafter). The containment vent is one of the accident management measures, and it can be expected to reduce the source terms of radioactive iodine and cesium if suppression pool bypass is avoided. This type of accident scenario is also meaningful from the viewpoint of clarifying the impact of radiation on people if the accident management measures work well.

In addition to these three severe accident scenarios, we calculated the average energy of gamma rays based on the release fractions from Fukushima Daiichi Nuclear Power Plant Units 1, 2, and 3 (NERHGJ, 2011). The inventories of radionuclides in the nuclear reactors as of shutdown were obtained from Nishihara (2012). The calculation results of average energy of gamma ray from the exposure pathway j, E_j, are shown as a function of time after shutdown in **Figs. 5a** and **b**. It is noted that these figures were drawn under the assumption that the release occurred immediately after reactor shutdown. However, in fact, a major release in the Fukushima accident occurred several days after the reactor shutdown. Therefore, the relative values of the released activities shown in **Table 2** are absolutely hypothetical and are to be used for evaluating the possible extent of average photon energy in nuclear accidents.

For cloudshine, the average energy of gamma rays ranged from 0.08 to 1.7 MeV, corresponding to various time phases after shutdown, as shown in **Fig. 5a**. Immediately after reactor shutdown, the average energy of gamma rays was dominated by contributions from short-lived radionuclides such as ^{87}Kr, ^{88}Kr, and radioactive iodine. In particular, the contribution of ^{88}Kr (E_i= 2.3 MeV) was the highest. For example, the contribution of ^{88}Kr to the average energy in Fukushima Unit 1, Unit 3, and TQUV-CV exceeded 60% immediately after shutdown. ^{88}Kr decayed with a half-life of 2.8 h, and its contribution to the average energy decreased rapidly. Thereafter, the contributions of ^{133}Xe (E_i = 0.055 MeV), radioactive iodine, and radioactive cesium increased gradually. Finally, after several days from shutdown, the average energy of gamma rays from cloudshine was around 0.4 MeV for all accident scenarios, except TQUV-CV and Fukushima Unit 2. In the case of Fukushima Unit 2, the contributions of ^{132}Te and its progeny nuclide ^{132}I (E_i = 0.55 MeV), ^{131}I (E_i = 0.37 MeV) and radioactive cesium were larger than those in other accident scenarios. Thus, the average energy of gamma rays was higher than that in the other accident scenarios. By contrast, the contribution of ^{133}Xe to the average energy of gamma rays in the TQUV-CV case exceeded 90% during the few days after shutdown, and this contribution was considerably higher than that in other accident scenarios. As a result, the average energy of gamma rays in The TQUV-CV case is lower than 0.1 MeV.

For groundshine, the average energy of gamma rays ranged from 0.58 to 0.91 MeV in various time phases after shutdown, as shown in **Fig. 5b**. Immediately after shutdown, the average energy was around 0.8–0.9 MeV in all accident scenarios. This is because the contribution of ^{135}I (E_i = 1.1 MeV) is dominant in this phase.

Thereafter, ^{135}I decayed with a half-life of 6.6 h, and the contributions of ^{131}I, ^{132}Te,^{134}Cs (E_i = 0.68 MeV), and ^{137}Cs (E_i=0.66 MeV) increased with time, and the average energy in each accident scenario continued to be around 0.6 MeV, which is the averaged value of the contributions of these radionuclides.

DRFs for vehicles in case of nuclear accident

Based on the considerations in the previous section, we decided to use the energy values of 0.4 MeV, 1 MeV, and 1.5 MeV for cloudshine. For groundshine, because the average energy of gamma rays due to the accident scenario and time-dependence was 0.6–0.8 MeV and then continued to be around 0.6 MeV, we used the average energy corresponding to ^{137}Cs. The DRFs shown in **Fig. 4** were evaluated by taking into account not only the contribution of ^{134}Cs but also those of ^{137}Cs. However, the contribution of ^{134}Cs is not considered in this section. As mentioned in the previous section, the average energies of ^{134}Cs and ^{137}Cs are almost similar, and the difference in DRFs between only ^{137}Cs, and both ^{134}Cs and ^{137}Cs are within about 1%. For these gamma ray energies, we evaluated the DRFs of vehicle models weighing 800–1930 kg (**Table 1**). The dose reduction effects are given by not only the steel body panel but also all other assemblies of a vehicle. The distribution of weight throughout the vehicle, including its heavy undercarriage/frame, dashboard, could provide shielding effects. Therefore, to take into account the dose reduction effects of these all assemblies, we used the thickness which were obtained from eqn (1) based on the weight of vehicle.

The evaluations for groundshine were performed based on the same calculation method and geometry as those described in the previous section. However, to consider the influence of photon source migration, a ^{137}Cs plane was set at the ground depth corresponding to the relaxation mass depths of 0 g cm^{-2}, 3 g cm^{-2}, 5 g cm^{-2}, 7.5 g cm^{-2}, and 10 g cm^{-2}. For cloudshine, the DRF evaluations were performed assuming submersion in a contaminated atmospheric cloud. In calculations of the ambient equivalent dose rate under air submersion, photon sources were located uniformly inside a half-sphere located above the ground and having a radius of 1000 m, which was filled with air. The calculations were performed under the assumption that the radioactive materials do not enter into the vehicle through ventilation or other pathways.

Tables 3a and **3b** show the DRF evaluation results of the vehicle models for cloudshine and for groundshine, respectively. As shown in **Table 3a**, the DRF of cloudshine for photon energies of 0.4 MeV, 1 MeV, and 1.5

MeV were 0.66–0.73, 0.78–0.85, and 0.82–0.88, respectively. The DRFs have a tendency to decrease with increasing vehicle model weight and decreasing photon energy. Immediately after shutdown, as shown in **Fig. 5a**, the average photon energy varies considerably. Thus, assessments of doses to persons in the vehicles must use DRFs after considering the variability in them. For groundshine, the DRFs were 0.64–0.73. These results were obtained under the assumption that ^{137}Cs is placed only on the ground surface. Therefore, if ^{137}Cs moves into the ground, these values are not applicable for dose assessments in such situation. To clarify the depth dependence of DRFs using the developed model, additional evaluations were made for β = 0.0 g cm^{-2}, 5.0 g cm^{-2}, and 10 g cm^{-2}. **Table 3b** shows the results of these evaluations. The results show that the DRFs obtained considering the migration of ^{137}Cs into the ground (β = 5 g cm^{-2}, 10 g cm^{-2}) are lower than those for ^{137}Cs only on the ground surface (β = 0 g cm^{-2}), and they decrease with increasing relaxation mass depth. The DRF for β = 0 g cm^{-2} was about 8% higher than that for β = 10 g cm^{-2} for each vehicle model. These results imply that the DRFs shown in **Table 3b** can be used to assess the doses conservatively even with the migration of ^{137}Cs into the ground.

In addition, we can point out that there is a difference of the DRF between for parts of person where there is glass and for parts of the person where there is steel panel. As described in calculation model for vehicle, the mass density thickness of the windows was lower than that for the steel body in our model. To evaluate the difference in the DRFs due to the difference in the mass density thickness between the windows and the steel plates, an additional detector was installed above the representative point at the same height of the center of the windows (**Fig. 3**). As an example, the DRFs of Vitz in this additional detector for cloudshine with photon energies of 0.4 MeV, 137Cs, 1.0 MeV, and 1.5 MeV were 9%, 7%, 6%, and 5% higher than those in the representative point. For groundshine from ^{137}Cs, the DRF in the additional detector were 8% higher than that in the representative point. Thus, if the DRFs are used for an assessment of equivalent dose for organs and tissues which are located in the height of windows, we have to consider this difference.

Compared to the previous study, Lauridsen and Hedemann (1983) reported that the DRFs due to European cars for uranium pellets from a commercial fuel element, and it ranged 0.58–0.72. These values were obtained from vehicles weighing 675–1350 kg. Because the radiation source and the experimental geometry are not the same between the two studies, it is difficult to compare the DRFs obtained in the present study with those

obtained by Lauridsen and Hedemann (1983). However, the tendency of DRF values is consistent between both studies, which means in both the studies, the DRFs decreased with increasing vehicle weight. In addition, the ranges of the DRFs in the two studies are similar. As a result, we can conclude that the model developed in this study can explain the measurement results from the previous study.

CONCLUSIONS

A vehicle model was developed based on the actual shape and weight of Japanese vehicles. The dose-reduction effects of vehicles were evaluated by calculating DRF, which is defined as the ratio of the ambient equivalent dose rate measured inside a vehicle to that measured at a height of 1 m above the ground in a large open field. We evaluated the DRFs not only by using the models but also by performing actual measurements. Good agreement was achieved between the modeled and the measured values. In addition, based on the developed vehicle models, we evaluated the DRFs for cloudshine and groundshine in the case of a nuclear accident. The evaluations were performed for the vehicle models weighing 800–1930 kg. Increasing vehicle weight was found to correlate with attenuation because the distribution of the weight throughout the vehicle may help shielding effect for cloudshine and goundshine. The DRFs for cloudshine with photon energies of 0.4 MeV, 1 MeV, and 1.5 MeV were 0.66–0.73, 0.78–0.85, and 0.82–0.88, respectively. The DRFs for cloudshine obtained in the present study should be used considering the variabilities due to photon energy from the radioactive plume and vehicle weight. For groundshine, the DRFs were 0.64–0.73. Although these results were evaluated under the assumption that ^{137}Cs is placed only on the ground surface, according to the results from our additional evaluations, the DRFs considering the migration of ^{137}Cs into the ground are lower than those for ^{137}Cs placed on the ground surface, and they decrease with increasing the relaxation mass depth. Consequently, even if ^{137}Cs migrates into the ground, doses to people in the vehicles considered herein can be assessed conservatively using the DRFs obtained in this study

ACKNOWLEDGEMENT

This work was part of the sheltering effect enhancement project, which was financed by the Nuclear Regulation Authority (NRA), Japan. The authors thank Dr. Kenzo Fujimoto and Mr. Jun Kawai (NRA) for their help and

expertise with environmental consequence assessment. In addition, the authors would also like to thank staffs of Tokyo Records Management Company Inc. for their supports in our experiments.

REFERENCES

Burson Z. G.and Profio A. E. Structure shielding in reactor accidents. *Health Phys*, **33**: 287–299; 1977.

Cutter S. and K. Barnes, Evacuation behavior and Three Mile Island, *Disasters*, **6**: 116–124; 1982.

Eckerman K. F. and J. C. Ryman, External exposure to radionuclides in air, water, and soil, Federal Guidance . Washington DC: Report No. 12, EPA-402-R-93-081; 1993.

Fukushima prefecture, Genshiryoku hatsudensyo syuhen kankyo hosyano sokutei kekka houkokusyo; 2010. Available at: http://www.pref.fukushima.lg.jp/uploaded/attachment/42296.pdf (accessed July 12 2017). (in Japanese)

Hiroi U., Investigation and analysis about the evacuation behavior from the Fukushima nuclear power plant, *Journal of the City Planning Institute of Japan*, **49**: 537–542; 2014. (in Japanese)

Homma T., J. Ishikawa, K. Tomita and K. Muramatsu, Radiological consequence assessments of degraded core accident scenarios derived from a generic level 2 PSA of a BWR. Ibaraki: JAERI-Research 2000-060; 2000.

IAEA, Generic Procedures for Assessment and Response during a Radiological Emergency, IAEA-TECDOC-1162; 2000.

ICRP, Conversion coefficients for use in radiological protection against external radiation, ICRP Publication 74, Annals of the ICRP, 26. No. 3–4; 1996.

JAEA, Analysis on dose reduction effects by using level 3 probabilistic safety assessment; 2012. Available at: https://www.nsr.go.jp/data/000058876.pdf (accessed 8 December 2016). (in Japanese)

Japan Radioisotope Association,Radioisotope pocket data book. Tokyo: Maruzen (2011). (in Japanese)

Ko Y. Introduction to vehicle material. Tokyo Denki University Press (2009). (in Japanese)

Lauridsen B. and Per-Hedemann J. Shielding factors for vehicles to γ radiation from activity deposited on structures and ground surfaces. *Health Phys*, **45**: 1039–1045; 1983.

Matsuda N. and K. Saito, Dojochu no houshasei sesiumu no sindo bunpu chosa,, Japan Atomic Energy Agency,part I.82–101; 2016. Available at: http://fukushima.jaea.go.jp/initiatives/cat03/entry08.html (accessed Dec 7 2016). (in Japanese)

Ministry of Environment,Kikan konnan chiiki ni okeru jyosen moderu jisho jigyo no kekka hokoku; 2014.

Available at: http://josen.env.go.jp/area/model2.html (accessed December 7 2016). (in Japanese)

NAIIC, The Official Report of The Fukushima Nuclear Accident Independent Investigation Commission, National Diet of Japan Fukushima Nuclear Accident Independent Investigation Commission. Tokyo: Tokuma Shoten; 2012. Available at: http://warp.da.ndl.go.jp/info:ndljp/pid/3856371/naiic.go.jp/en/report/ (accessed 13 December, 2016)

Nuclear Emergency Response Headquarters Governmentof Japan. Report of Japanese Government to the IAEA Ministerial Conference on Nuclear Safety—The Accident TEPCO's Fukushima Nuclear Power Station—,Attachment IV-2: The Cross Check Analysis on the Evaluation of the Cores of Unit 1, 2 and 3 of Fukushima Dai-ichi NPP reported by TEPCO; 2011.Available at: http://japan.kantei.go.jp/kan/topics/201106/pdf/attach_04_2.pdf. (Accessed December 2 2016)

Nishihara K., H. Iwamoto and K. Suyama.Estimation of Fuel Compositions in Fukushima-Daiichi Nuclear Power Plant, JAEA-Data/Code 2012-018. Ibaraki: JAEA ; 2012. (in Japanese)

OECD/NEA/CRPPH, International Short-Term Countermeasures Survey 2012 Update, OECD/NEA/CRPPH/R(2013)4; 2013. Available at: https://www.oecd-nea.org/rp/docs/2013/crpph-r2013-4.pdf (Accessed 31 October, 2017)

UNSCEAR. UNSCEAR 2013 Report, Volume 1, Report to the General Assembly, Scientific Annex A: Levels and effects of Raditaion exposure due to the nuclear accident after the 2011 great east-Japan earthquake and tsunami, United Nations Scientific Committee on the Effects of Atomic Radiation. New York: United Nations; 2014.

U.S. Environmental Protection Agency. External Exposure to Radionuclides inAir, Water, and Soil, Federal Guidance Report No. 12, EPA-402-R-93-081; 1993.

White M. C., Photoatomic Data Library MCPLIB04: A New Photoatomic Library Based On Data from ENDF/B-VI Release 8, LA-UR-03-1019, Los Alamos; 2003.

X-5 Monte Carlo Team, MCNP–A General Monte Carlo N-Particle Transport Code, Version 5 Volume I: Overview and Theory, LA-UR-03-1987, Los Alamos; 2003.

Footnote

* All of the prefectures with nuclear power plant (Hokkaido, Aomori, Miyagi, Fukushima, Ibraki, Niigata, Shizuoka, Ishikawa, Fukui, Shimane, Ehime, Saga, Kagoshima) formally state that self-evacuation by a private vehicle is one of the typical method for wide-area evacuationin their local management plan. All of these plans were established after the Fukushima accident taking into actual experiences of the public evacuation in the accident.

** Personal Communication, Honda Motor Co., Ltd., 8-1 Moto-Machi, Wako, Saitama, Japan; 5 November 2015.

List of figures

List of tables

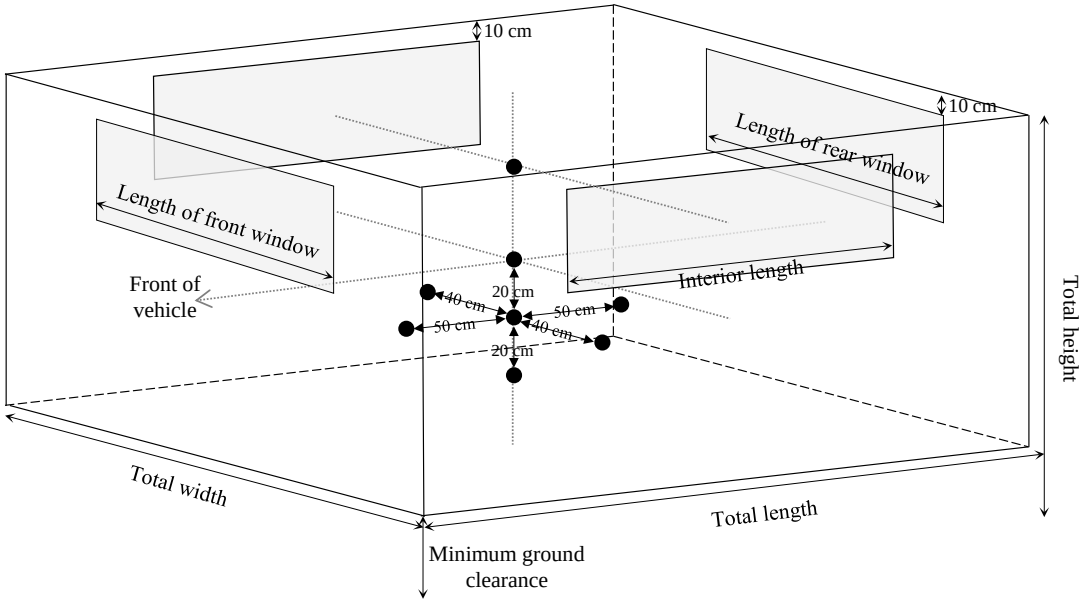

Fig.1. Schematic illustration of vehicle model and detector position

Fig.2. Overhead view of measurement location in Futaba Town

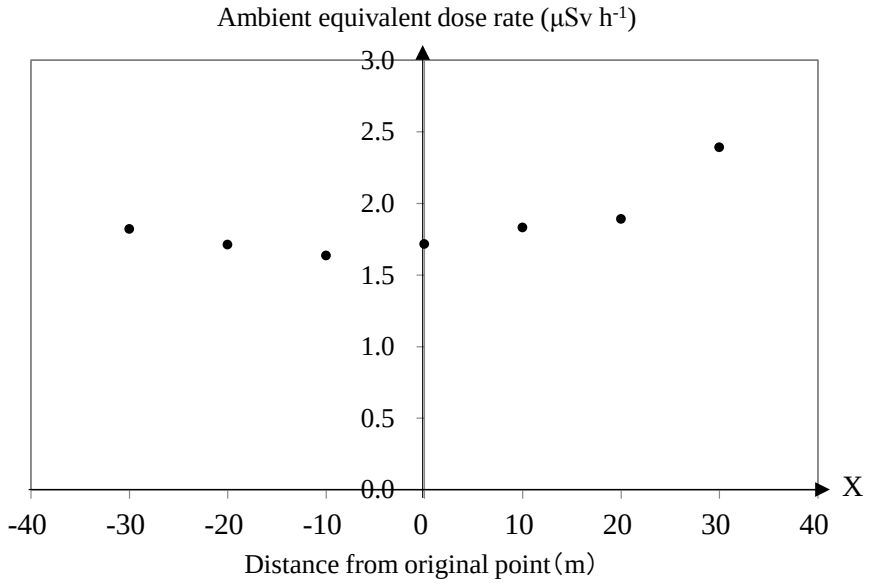

(a) Ambient equivalent dose rate along X-axis in Fig.2.

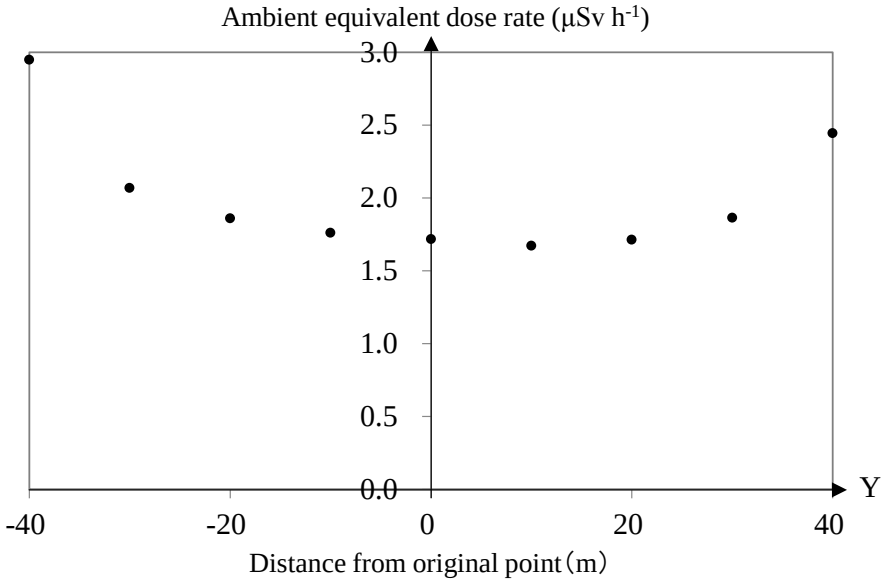

(b) Ambient equivalent dose rate along Y-axis in Fig. 2.

Fig.3. Radiation characteristics at measurement location

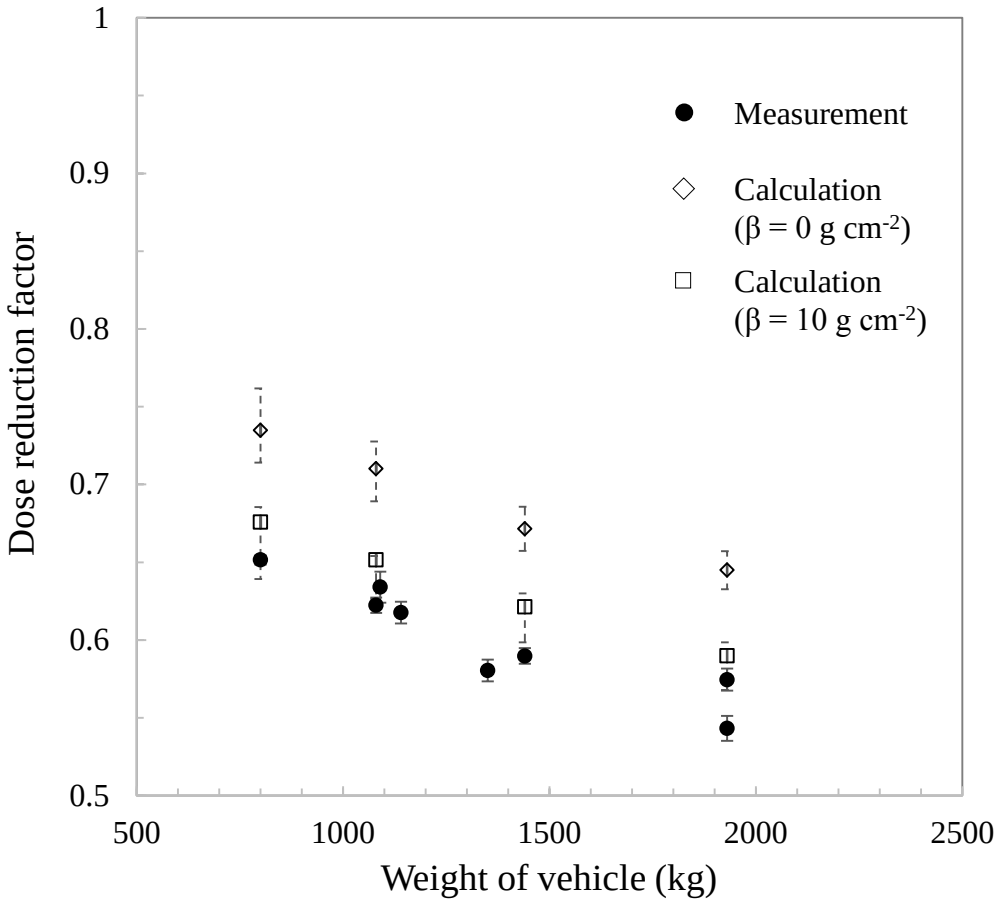

Fig.4. Dose-reduction factors of vehicle based on actual measurements and calculations

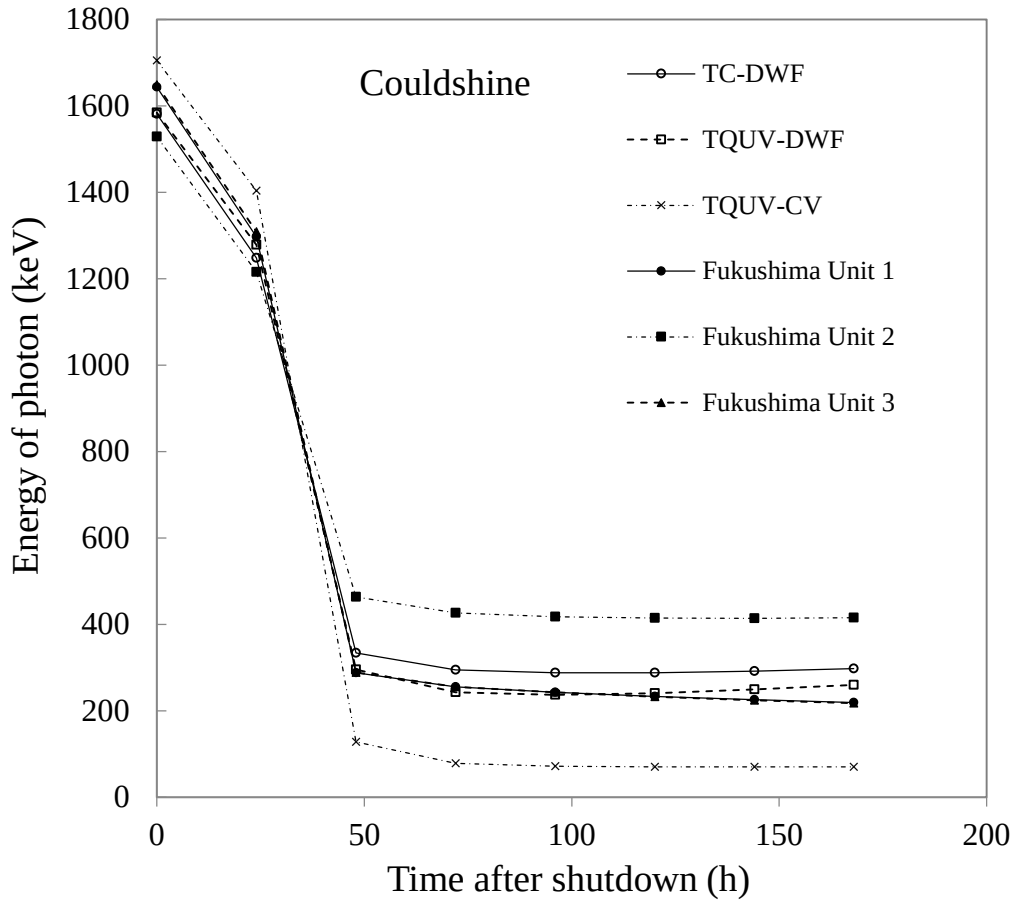

Fig.5a. Time dependence of average energy of photon from cloudshine in case of nuclear accident

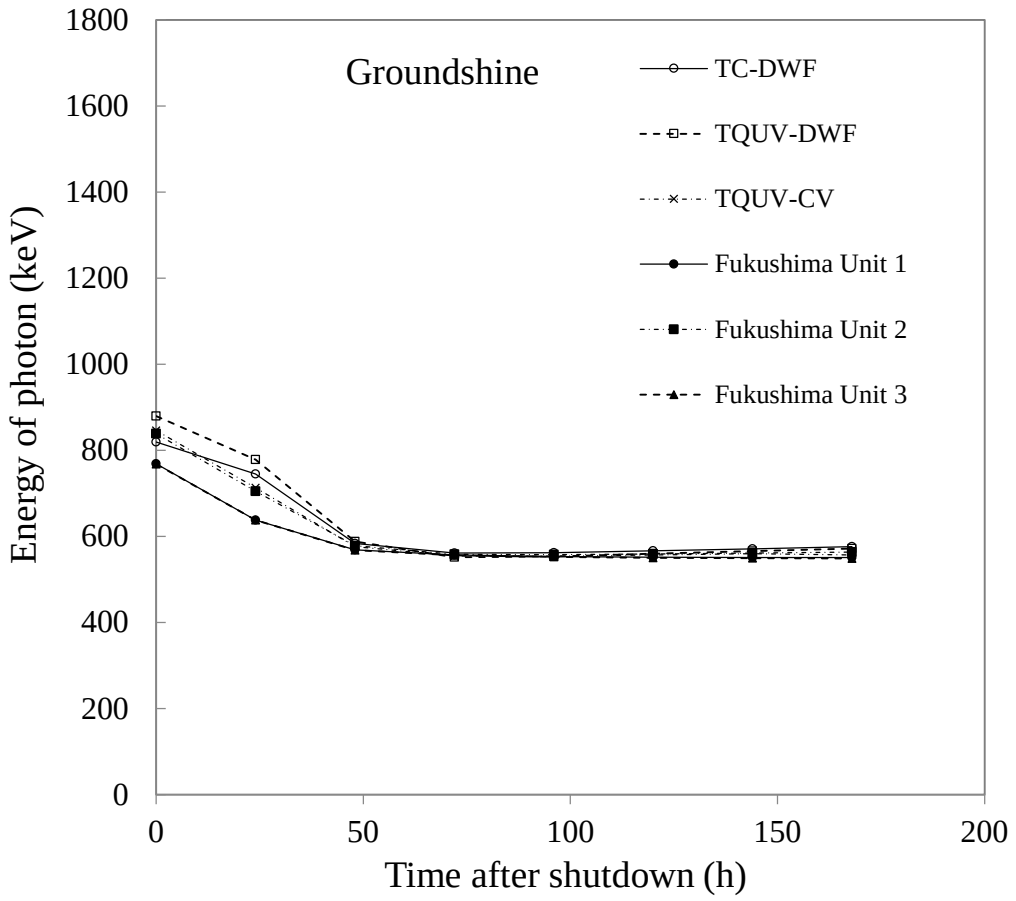

Fig. 5b. Time dependence of average energy of photon from groundshine in case of nuclear accident

Table 1 Vehicles used for development of a model

	Mira	Vitz	Wish	Alphard
Weight (kg)	800	1080	1440	1930
Total length (mm)	3390	3885	4590	4870
Total width (mm)	1470	1695	1720	1830
Total height (mm)	1530	1530	1600	1900
Minimum ground clearance (mm)	160	140	150	160
Interior length (mm)	2000	1920	2660	3210
Length of front and rear window(mm)	1270	1298	1520	1630
Height of window(mm)[a]	404	418	421	440
Thickness of vehicle body (mm)[b]	0.703	0.780	0.856	0.929

[a] Height of window was obtained as averaged value of height of four windows (front, rear, and side).

[b]Thickness values shown in this table were evaluated based on the weight and the areas of the body surface taking into account: (i) ceiling thickness of 0.08 cm, and (ii) correction related to actual vehicle shape. The actual shape of vehicle body is not rectangular because the corners of vehicle body are rounded, and the vehicle body has a slope to allow drivers and passengers to see the outside from the inside. We corrected the surface areas of vehicle body taking into account these aspects.

Table 2 Relative value of released activity for each accident scenario

Radionuclide	Relative value of released activity A_i for each accident scenario					
	TC-DWF	TQUV-DWF	TQUV-CV	Fukushima Unit 1	Fukushima Unit 2	Fukushima Unit 3
^{85m}Kr	7.68×10^{1}	7.68×10^{1}	2.67×10^{3}	8.64×10^{2}	5.93×10^{1}	1.29×10^{3}
^{87}Kr	1.48×10^{2}	1.48×10^{2}	5.07×10^{3}	1.24×10^{3}	8.67×10^{1}	1.86×10^{3}
^{88}Kr	2.14×10^{2}	2.14×10^{2}	7.33×10^{3}	1.69×10^{3}	1.20×10^{2}	2.57×10^{3}
^{133}Xe	6.07×10^{2}	6.07×10^{2}	2.07×10^{4}	4.41×10^{3}	3.00×10^{2}	6.29×10^{3}
^{135}Xe	1.71×10^{2}	1.71×10^{2}	5.87×10^{3}	1.69×10^{3}	1.00×10^{-7}	2.29×10^{3}
^{95}Zr[a]	1.00×10^{-4}	3.39×10^{-9}	1.27×10^{-7}	4.24×10^{-4}	1.93×10^{-4}	6.29×10^{-4}
^{95}Nb	1.02×10^{-4}	3.39×10^{-9}	1.33×10^{-7}	3.73×10^{-4}	1.60×10^{-4}	5.57×10^{-4}
^{99}Mo[b]	2.68×10^{-4}	2.14×10^{-8}	7.33×10^{-7}	3.90×10^{-6}	1.60×10^{-7}	5.71×10^{-6}
^{103}Ru[c]	2.32×10^{-4}	1.79×10^{-8}	6.13×10^{-7}	2.88×10^{-6}	1.07×10^{-7}	4.14×10^{-6}
^{127}Sb	2.32×10^{-1}	9.64×10^{-3}	3.93×10^{-1}	8.64×10^{-1}	1.53×10^{0}	3.00×10^{0}
^{131}I	9.46×10^{0}	1.02×10^{1}	1.07×10^{1}	1.51×10^{1}	1.07×10^{1}	2.14×10^{1}
^{133}I	1.96×10^{1}	2.14×10^{1}	2.13×10^{1}	3.22×10^{1}	2.20×10^{1}	4.57×10^{1}
^{134}I	2.14×10^{1}	2.32×10^{1}	2.33×10^{1}	3.56×10^{1}	2.47×10^{1}	5.14×10^{1}
^{135}I	1.79×10^{1}	1.96×10^{1}	2.00×10^{1}	3.05×10^{1}	2.07×10^{1}	4.43×10^{1}
^{131}Te	3.04×10^{-1}	1.32×10^{-2}	5.40×10^{-1}	5.76×10^{0}	1.07×10^{0}	8.43×10^{0}
^{132}Te[d]	3.04×10^{0}	1.29×10^{-1}	5.27×10^{0}	3.56×10^{1}	6.67×10^{0}	5.29×10^{1}
^{134}Cs	1.18×10^{0}	1.18×10^{0}	1.20×10^{0}	9.32×10^{-1}	1.07×10^{0}	1.04×10^{0}
^{136}Cs	4.11×10^{-1}	4.11×10^{-1}	4.07×10^{-1}	2.71×10^{-1}	3.13×10^{-1}	3.43×10^{-1}
^{137}Cs	1.00	1.00	1.00	1.00	1.00	1.00
^{140}Ba[e]	3.75×10^{-2}	8.75×10^{-6}	4.07×10^{-4}	1.69×10^{-1}	7.33×10^{-2}	2.43×10^{-1}
^{239}Np	1.23×10^{-3}	4.11×10^{-8}	1.60×10^{-6}	5.08×10^{-9}	1.67×10^{-9}	4.86×10^{-9}

Note: The values shown in this table are normalized by ^{137}Cs activity in each accident scenario. All of them were calculated as the product of reactor inventory as of the shutdown and the release fraction of radionuclides.

[a]Includes contribution of ^{95m}Nb, [b]Includes contribution of ^{99m}Tc, [c]Includes contribution of ^{103m}Rh, [d]Includes contribution of ^{132}I, [e]Includes contribution of ^{140}La.

Table 3a Dose-reduction factors of vehicle model for cloudshine

Vehicle model		Dose reduction factor for various photon energies		
Type	Weight (kg)	0.4 MeV	1 MeV	1.5 MeV
Mira	800	0.73 ± 0.028	0.85± 0.027	0.88± 0.020
Vitz	1080	0.72 ± 0.029	0.84± 0.023	0.87± 0.018
Wish	1440	0.71 ± 0.028	0.83± 0.024	0.86± 0.020
Alphard	1930	0.66± 0.034	0.78± 0.026	0.82± 0.021

Table 3b Dose-reduction factors of vehicle model for groundshine

Vehicle model		Dose reduction factor for relaxation mass depth[a]		
Type	Weight (kg)	0 g cm^{-2}	5 g cm^{-2}	10 g cm^{-2}
Mira	800	0.73± 0.018	0.69 ± 0.018	0.67 ± 0.017
Vitz	1080	0.70± 0.012	0.66 ± 0.014	0.65 ± 0.012
Wish	1440	0.66 ± 0.009	0.64 ± 0.014	0.62 ± 0.013
Alphard	1930	0.64 ± 0.008	0.60 ± 0.012	0.59 ± 0.012